Siting and Sizing of DG Units Considering Energy Equity: Model, Solution, and Guidelines

Chenchen Li, *Graduate Student Member, IEEE*, Fangxing Li, *Fellow, IEEE*, Sufan Jiang, *Member, IEEE*, Xiaofei Wang, *Member, IEEE*, and Jinning Wang, *Graduate Student Member, IEEE*

***Abstract*—Low-income communities have challenges obtaining equal access to electricity, so it is important to implement energy justice. Meanwhile, increasing installations of distributed generators (DGs) in distribution systems is a viable means to promote energy equity. Therefore, this work explores a new planning method to address the siting and sizing problem of DG units with an energy equity constraint embedded in the model, and provides concluding guidelines as a rule of thumb for future DG planning considering energy equity. In this paper, first, the DG siting and sizing problem is formulated as a stochastic bi-level model, where energy equity is considered as an energy burden constraint. The upper level determines the optimal sites and sizes of DGs under investment and energy burden constraints, while the lower level optimizes the distribution operation. Next, a solution method is proposed by applying the Karush-Kuhn-Tucker optimality conditions to convert the stochastic bi-level model to a single-level model. A decomposition approach and Progressive Hedging Algorithm are used to further simplify the single-level model into multiple easy-to-solve subproblems. Finally, numerical studies are performed on two test systems to verify the effectiveness of the proposed model. Technical rule-of-thumb guidelines are presented for siting and sizing DGs considering energy equity.**

***Index Terms*—Distributed generator (DG), energy burden, energy equity, Progressive Hedging Algorithm (PHA), siting and sizing, stochastic bi-level model.**

NOMENCLATURE

Abbreviations

DG	Distributed Generator
DLMP	Distribution Locational Marginal Price
KKT	Karush-Kuhn Tucker
LMP	Locational Marginal Price
MEB	Minimum Energy Burden
MINLP	Mixed-Integer Nonlinear Programming
PHA	Progressive Hedging Algorithm
SMIP	Stochastic Mixed-integer Programming

Sets

Ω_H	Set of households in a distribution system
Ω_T	Set of time intervals in a day
Ω_S	Set of scenarios
Ω_N	Set of buses
Ω_L	Set of lines
Ω_G	Set of DGs
Ω_{SC}	Set of shunt capacitors
Ω_{LH}	Set of low-income households

Constants

$P_{i,t}^{D,s}/Q_{i,t}^{D,s}$	Active/reactive load demand of bus i at time t
I_i	Annual income of household i
ρ_s	Probability of scenario s
$P_{\max}^{DG}$	Maximum rated power of DGs to be installed
N_{DG}	Maximum number of DGs to be installed
c_{dg}	Investment budget for the DG installation
e_i^0	Energy burden criterion of household i
$\sigma_{Sub,t}^{P,s}/\sigma_{Sub,t}^{Q,s}$	Active/reactive LMP of the substation at time t
$\sigma_{i,t}^{P,s}/\sigma_{i,t}^{Q,s}$	Active/reactive bidding price of DG i at time t
$V_{Sub,t}^{s}$	Bus voltage of the substation at time t
$V^{\min}/V^{\max}$	Minimum/maximum bus voltage
$P_i^{G,\min}$	Minimum active power of DG i
$Q_i^{G,\min}/Q_i^{G,\max}$	Minimum/maximum reactive power of DG i
θ_i	Power factor of DG i

Variables

e_i	Energy burden of household i
$\pi_{i,t,s}$	Active DLMP of bus i at time t
P_i^R	Rated power of DG installed at bus i
k_i	Binary variable indicating whether a DG is installed at bus i
$P_t^{L,s}/Q_t^{L,s}$	Active/reactive power loss at time t
$P_{Sub,t}^{G,s}/Q_{Sub,t}^{G,s}$	Active/reactive power come from utility grid at time t
$P_{i,t}^{G,s}/Q_{i,t}^{G,s}$	Active/reactive power of DG i at time t
$V_{i,t}^{s}$	Bus voltage of bus i at time t
r_l/x_l	Reactance/inductance of line l
$\lambda_t^{P,s}/\lambda_t^{Q,s}$	Lagrangian multipliers associated with active/reactive power balance constraints

Manuscript received 30 August 2023; revised 7 December 2023; accepted 1 January 2024. Date of publication 8 January 2024; date of current version 21 June 2024. This work was supported in part by the CURENT Research Center. Paper no. TSG-01390-2023. *(Corresponding author: Fangxing Li.)*

The authors are with the Department of EECS, The University of Tennessee, Knoxville, TN 37996 USA (e-mail: fli6@utk.edu).

Color versions of one or more figures in this article are available at https://doi.org/10.1109/TSG.2024.3350914.

Digital Object Identifier 10.1109/TSG.2024.3350914

$\omega_{i,t}^{(\cdot)\min,s}/\omega_{i,t}^{(\cdot)\max,s}$	Lagrangian multipliers associated with inequity of bus voltage and active/reactive power constraints
$\kappa_{i,t}^{-,s}/\kappa_{i,t}^{+,s}$	Lagrangian multipliers associated with inequity of reactive power constraints

I. Introduction

NEW ENERGY infrastructure and energy projects, if not well coordinated with social justice perspectives, may increase the cost of using electricity for households [1]. For example, the increasing electricity price in California has affected the proportion of household's various living expenses and reduced their disposable income [2]. What's worse, this phenomenon is especially noteworthy in low-income households, and the high energy burden even leads to them being unable to use electricity the same way as they used to. In other words, because of the difference in energy burden, households with different incomes have unequal access to electricity. As such, energy equity is highly important to consider in the developing new energy infrastructure and energy projects [3].

Energy equity can be defined as the fair production, distribution, and use of energy. For households buying electricity from the utility, energy equity means that they have access to affordable electricity. However, many households lack access to affordable electricity due to low income, which greatly affects their living quality. It is estimated that more than 5.2 million households above the Federal Poverty Line in the U.S. spend a significant portion of their income on energy [4]. To make matters worse, many low-income households struggle to access electricity to meet their basic needs [5]. In 2010, 19822 emergency room visits in 14 states of the U.S. resulted from heat stroke due to lack of air conditioning and outdoor exposure, and low-income people in rural area accounts for the majority [6]. The struggle of low-income households to secure basic electricity became particularly obvious during the COVID-19 pandemic [7], [8], [9].

To address the above problems, some countries have proposed or enacted policies to benefit low-income households. The U.K. has proposed a metric considering multiple factors to determine the level of support needed by households [10]. In the U.S., there are two main energy assistance programs, the Low Income Home Energy Assistance Program and the Weatherization Assistance Program [11], [12]. In addition, policies enacted in 2021 in Oregon and Illinois require utilities to outline distribution grid investments befitting low-income and disproportionately impacted communities [13], [14].

There are a few technical papers in the literature studying methods to realize energy equity at the distribution side. A method to quantify the equity on energy expenditure has been proposed [15], and a bilevel optimization problem was built to obtain the optimal design of retail electricity tariffs [16]. For realizing the equity of power curtailment among photovoltaic owners, a method that weights power curtailment based on the return-on-investment value has been proposed [17]. In the peer-to-peer energy trading framework, an on-demand share allocation transfer model has been established to improve energy equity [18]. A quantitative framework has also been proposed to support policy decision-making around equitable energy interventions, where three interventions are considered, weatherization intervention, the deployment of rooftop solar, and the deployment of community-owned renewable generation [19].

As mentioned in [19], the deployment of distributed generator (DG) units can be an effective way to realize energy equity in distribution operation, because DG units can affect the net electricity demand. Also, different operational strategies of DG units can lead to different electricity prices. However, there is no discussion of proper planning approaches to site and size DGs considering energy justice.

In traditional DG planning, a critical step is to identify the best locations and sizes of DG units. This is also called the DG siting and sizing problem, commonly based on a mixed integer programming model that can be further divided into single-objective model [20], [21] and multiple-objective model [22], [23]. The single-objective model typically considers power losses, voltage profile, investment cost, load shedding, or carbon emission, while the multi-objective model considers permutations and combination of various single objectives.

Although the above models and methods succeed under certain scenarios, the effectiveness of installing DG units to achieve energy equity represents a gap in the literature. As DGs are installed close to end consumers, they can be highly effective in implementing energy equity in low-income communities. With this motivation, in this work, we consider energy equity in the planning problem of DG siting and sizing. The contributions are summarized as follows:

- High-level planning guidelines are obtained for the DG siting and sizing problem to better achieve energy equity.
- A stochastic bi-level model considering energy equity in a quantitative manner is proposed for siting and sizing DG units, where the upper level minimizes the power losses and satisfies investment cost and energy equity constraints, and the lower level minimizes the generation cost and meets the operational constraints.
- A solution method is proposed to solve the stochastic bi-level model, which combines Karush-Kuhn Tucker (KKT) optimality conditions, time decomposition, and Progressive Hedging Algorithm (PHA). The KKT optimality conditions convert the bi-level model to a single-level model. Then, the time decomposition method and PHA simplify the single-level model into multiple easy-to-solve subproblems, reducing the dimension of the problem and the requirements of computation resources.

The rest of the paper is organized as follows. Section II proposes the stochastic bi-level model for the DG siting and sizing problem with energy equity constraints considered. Section III describes the scenario extraction methods. Section IV proposes the solution methods via PHA. Section V presents case studies, and guidelines to improve energy equity via DG planning are summarized and discussed. Section VI concludes this paper.

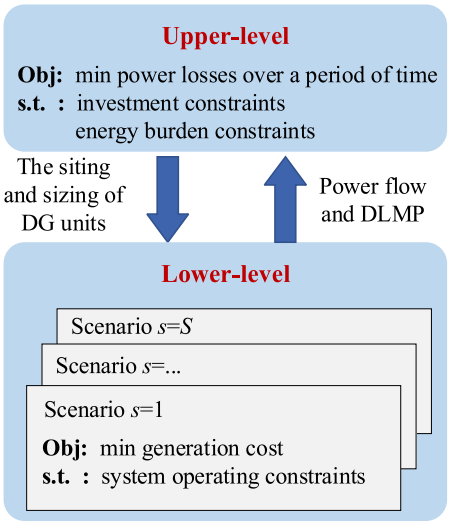

Fig. 1. Framework of the proposed stochastic bi-level model.

II. Stochastic Bi-Level Model for DG Siting and Sizing With Energy Equity Constraint

It is well understood that the location and size of a new DG unit may have an impact on power losses, voltages, generation costs and operation conditions. Thus, it is necessary to employ a method to evaluate DG's economic impact without violating technical constraints. Here, the distribution locational marginal price (DLMP) method is used to model the price at each node, since the DLMP is of significant interest for modeling future competitive distribution or local markets. Based on the DLMP, a stochastic bi-level model is proposed to site and size DG units in a distribution network while the energy equity constraints, as well as all typical technical constraints, are considered. The overall framework is shown in Fig. 1. It should be noted that the proposed model is based on a typical distribution feeder configuration. If distribution reconfiguration during emergency must be considered in a planning problem (e.g., for an area prone to extreme weather), it will add much higher complexity to the problem to solve, and a potential solution may relax the steady-state model while including reconfiguration considerations.

A. Quantitative Model of Energy Equity

Unequal access to electricity is a manifestation of energy inequity. In this characteristic, energy burden is used to quantify the energy equity in this paper. Energy burden is the percentage of household income spent on energy costs, representing the ability to obtain reliable energy [24]. The mathematical model is shown as follows.

$$e_i = \sum_{s\in\Omega_S}\sum_{t\in\Omega_T}\frac{\pi_{i,t,s}\cdot P_{i,t}^{D,s}}{I_i},\ i\in\Omega_H \tag{1}$$

B. Upper-Level Model

The upper-level model minimizes the power losses of a distribution system while satisfying both the investment constraints of DG units and the energy burden constraints. The decision variables are the DGs' location and capacity, i.e., $\boldsymbol{x} = (P_i^R, k_i), i\in\Omega_N$.

$$min\ 365\cdot\sum_{s\in\Omega_S}\sum_{t\in\Omega_T}\rho_s\cdot P_t^{L,s} \tag{2}$$

$$s.t.\ 0\le P_i^R\le P_{\max}^{DG}\cdot k_i,\forall i\in\Omega_N \tag{3}$$

$$0\le\sum_{i\in\Omega_N}k_i\le N_{DG},\forall i\in\Omega_N \tag{4}$$

$$\sum_{i\in\Omega_N}\alpha\cdot P_i^R+\beta\cdot k_i\le c_{dg} \tag{5}$$

$$365\cdot\sum_{s\in\Omega_S}\sum_{t\in\Omega_T}\rho_s\cdot\frac{\pi_{i,t,s}\cdot P_{i,t}^{D,s}}{I_i}\le e_i^0,\forall i\in\Omega_H \tag{6}$$

where (3) is the DG units capacity constraint, which is related to the binary variable k_i. If there is no DG unit installed at the bus i, the rated power of the DG unit will be 0; otherwise, the DG output can be between 0 and its maximum rated power. Equation (4) limits the number of installed DG units. The investment budget of DG units is limited by (5), which is modeled as a linear function representing variable and fixed cost. Also, α and β in (5) are the constant parameters related to investment cost [22], [25]. Further, the investment costs of DG units are undertaken by utility companies. Equation (6) represents the energy burden constraint at each bus.

C. Lower-Level Model

The lower-level model optimizes the distribution system operation, minimizing the system generation cost while satisfying the operational constraints.

$$min\ \sum_{t\in\Omega_T}\left(\sigma_{Sub,t}^{P,s}\cdot P_{Sub,t}^{G,s}+\sigma_{Sub,t}^{Q,s}\cdot\widehat{Q}_{Sub,t}^{G,s}+\sum_{i\in\Omega_G}\left(\sigma_{i,t}^{P,s}\cdot P_{i,t}^{G,s}+\sigma_{i,t}^{Q,s}\cdot\widehat{Q}_{i,t}^{G,s}\right)\right) \tag{7}$$

$$s.t.\ P_{Sub,t}^{G,s}+\sum_{i\in\Omega_G}P_{i,t}^{G,s}-\sum_{i\in\Omega_N}P_{i,t}^{D,s}-P_t^{L,s}=0:\lambda_t^{P,s} \tag{8}$$

$$Q_{Sub,t}^{G,s}+\sum_{i\in\Omega_G}Q_{i,t}^{G,s}-\sum_{i\in\Omega_N}Q_{i,t}^{D,s}-Q_t^{L,s}=0:\lambda_t^{Q,s} \tag{9}$$

$$V_{i,t}^s=V_{Sub,t}^s+\sum_{j\in\Omega_N}Z_{i,j}^P\cdot\left(P_{j,t}^{G,s}-P_{j,t}^{D,s}\right)+\sum_{j\in\Omega_N}Z_{i,j}^Q\cdot\left(Q_{j,t}^{G,s}-Q_{j,t}^{D,s}\right),\forall i\in\Omega_N \tag{10}$$

$$V^{\min}\le V_{i,t}^s\le V^{\max}:\omega_{i,t}^{v\min,s},\omega_{i,t}^{v\max,s},\forall i\in\Omega_N \tag{11}$$

$$P_i^{G,\min}\le P_{i,t}^{G,s}\le P_i^R:\omega_{i,t}^{P\min,s},\omega_{i,t}^{P\max,s},\forall i\in\Omega_G \tag{12}$$

$$Q_i^{G,\min}\le Q_{i,t}^{G,s}\le P_{i,t}^{G,s}\cdot\tan(\arccos\theta_i):\omega_{i,t}^{Q\min,s},\omega_{i,t}^{Q\max,s},\ \forall i\in\Omega_G \tag{13}$$

$$Q_i^{G,\min}\le Q_{i,t}^{G,s}\le Q_i^{G,\max}:\omega_{i,t}^{Q\min,s},\omega_{i,t}^{Q\max,s},\forall i\in\Omega_{SC} \tag{14}$$

$$-Q_{i,t}^{G,s}\le\widehat{Q}_{i,t}^{G,s},Q_{i,t}^{G,s}\le\widehat{Q}_{i,t}^{G,s}:\kappa_{i,t}^{-,s},\kappa_{i,t}^{+,s},\forall i\in\Omega_G \tag{15}$$

where (8) and (9) are the active and reactive power balance constraints. Equation (10) is the voltage equation, which is derived from linearized power flow for a distribution

system [26], [27]. In the voltage equation, $Z^P_{i,j}$ and $Z^Q_{i,j}$ are the bus voltage change coefficients related to net active and reactive power injection. Equation (11) is the bus voltage constraint. Equations (12) - (15) are the active and reactive power output constraints. Note, the reason for $\widehat{Q}^{G,s}_{i,t} = |Q^{G,s}_{i,t}|$ is that there is a cost to absorbing and generating reactive power [28].

Based on (7) – (15), the Lagrangian function can be written as (16). The DLMP is the first-order partial derivative of the Lagrangian function with respect to the active power, as shown in (17). The DLMP will be employed to calculate the consumer payment and then the energy burden.

$$
\begin{aligned}
L = \sum_{t\in\Omega_T}\Bigg(&\sigma^{P,s}_{Sub,t}\cdot P^{G,s}_{Sub,t} + \sigma^{Q,s}_{Sub,t}\cdot \widehat{Q}^{G,s}_{Sub,t} \\
&+ \sum_{i\in\Omega_G}\left(\sigma^{P,s}_{i,t}\cdot P^{G,s}_{i,t} + \sigma^{Q,s}_{i,t}\cdot \widehat{Q}^{G,s}_{i,t}\right)\Bigg) \\
&- \sum_{t\in\Omega_T}\lambda^{P,s}_t\cdot\left(P^{G,s}_{Sub,t} + \sum_{i\in\Omega_G}P^{G,s}_{i,t} - \sum_{i\in\Omega_N}P^{D,s}_{i,t} - P^{L,s}_t\right) \\
&- \sum_{t\in\Omega_T}\lambda^{Q,s}_t\cdot\left(Q^{G,s}_{Sub,t} + \sum_{i\in\Omega_G}Q^{G,s}_{i,t} - \sum_{i\in\Omega_N}Q^{D,s}_{i,t} - Q^{L,s}_t\right) \\
&- \sum_{t\in\Omega_T}\sum_{i\in\Omega_N}\omega^{v\min,s}_{i,t}\cdot\left(V^s_{i,t} - V^{\min}\right) - \sum_{t\in\Omega_T}\sum_{i\in\Omega_N}\omega^{v\max,s}_{i,t} \\
&\cdot\left(V^{\max} - V^s_{i,t}\right) \\
&- \sum_{t\in\Omega_T}\sum_{i\in\Omega_G}\omega^{P\min,s}_{i,t}\cdot\left(P^{G,s}_{i,t} - P^{G,\min}_i\right) - \sum_{t\in\Omega_T}\sum_{i\in\Omega_G}\omega^{P\max,s}_{i,t} \\
&\cdot\left(P^R_i - P^{G,s}_{i,t}\right) \\
&- \sum_{t\in\Omega_T}\sum_{i\in\Omega_G}\omega^{Q\min,s}_{i,t}\cdot\left(Q^{G,s}_{i,t} - Q^{G,\min}_i\right) \\
&- \sum_{t\in\Omega_T}\sum_{i\in\Omega_G}\omega^{Q\max,s}_{i,t}\cdot\left(P^{G,s}_{i,t}\cdot\tan(\arccos\theta_i) - Q^{G,s}_{i,t}\right) \\
&- \sum_{t\in\Omega_T}\sum_{i\in\Omega_{SC}}\omega^{Q\min,s}_{i,t}\cdot\left(Q^{G,s}_{i,t} - Q^{G,\min}_i\right) - \sum_{t\in\Omega_T}\sum_{i\in\Omega_{SC}}\omega^{Q\max,s}_{i,t} \\
&\cdot\left(Q^{G,\max}_i - Q^{G,s}_{i,t}\right) \\
&- \sum_{t\in\Omega_T}\sum_{i\in\Omega_G}\kappa^{-,s}_{i,t}\cdot\left(\widehat{Q}^{G,s}_{i,t} + Q^{G,s}_{i,t}\right) - \sum_{t\in\Omega_T}\sum_{i\in\Omega_G}\kappa^{+,s}_{i,t} \\
&\cdot\left(\widehat{Q}^{G,s}_{i,t} - Q^{G,s}_{i,t}\right) \qquad (16)
\end{aligned}
$$

$$
\begin{aligned}
\pi^s_{i,t} = \lambda^{P,s}_t + \lambda^{P,s}_t\cdot\frac{\partial P^{L,s}_t}{\partial P^{D,s}_{i,t}} + \lambda^{Q,s}_t\cdot\frac{\partial Q^{L,s}_t}{\partial P^{D,s}_{i,t}} \\
+ \sum_{j\in\Omega_N}\left(\omega^{v\min,s}_{j,t} - \omega^{v\max,s}_{j,t}\right)\cdot Z^P_{j,i},\ \forall i\in\Omega_N \qquad (17)
\end{aligned}
$$

In (17), the first-order partial derivative of the active power losses and reactive power losses w.r.t. the active power can be written as (18) and (19) [28]. According to the power flow calculation, the branch power losses $P^{L,s}_{l,t}$ and $Q^{L,s}_{l,t}$ can be calculated by (20) and (21) [29]. Then, the first-order partial derivative of the active and reactive branch power losses w.r.t. the active power can be expressed as (22) and (23).

$$\frac{\partial P^{L,s}_t}{\partial P^{D,s}_{i,t}} = \sum_{l\in\Omega_L}\frac{\partial P^{L,s}_{l,t}}{\partial P^{D,s}_{i,t}},\ \forall i\in\Omega_N \qquad (18)$$

$$\frac{\partial Q^{L,s}_t}{\partial P^{D,s}_{i,t}} = \sum_{l\in\Omega_L}\frac{\partial Q^{L,s}_{l,t}}{\partial P^{D,s}_{i,t}},\ \forall i\in\Omega_N \qquad (19)$$

$$P^{L,s}_{l,t} = \frac{\left(P^{F,s}_{l,t}\right)^2 + \left(Q^{F,s}_{l,t}\right)^2}{V^2_{l\_e,t}}\cdot r_l,\ \forall l\in\Omega_L \qquad (20)$$

$$Q^{L,s}_{l,t} = \frac{\left(P^{F,s}_{l,t}\right)^2 + \left(Q^{F,s}_{l,t}\right)^2}{V^2_{l\_e,t}}\cdot x_l,\ \forall l\in\Omega_L \qquad (21)$$

$$\frac{\partial P^{L,s}_{l,t}}{\partial P^{D,s}_{i,t}} = \left(2\cdot P^{F,s}_{l,t}\cdot S^{F_P,s}_{l,t} + 2\cdot Q^{F,s}_{l,t}\cdot S^{F_Q,s}_{l,t}\right)\cdot\frac{r_l}{V^2_{l\_e,t}},\quad \forall i\in\Omega_N,\forall l\in\Omega_L \qquad (22)$$

$$\frac{\partial Q^{L,s}_{l,t}}{\partial P^{D,s}_{i,t}} = \left(2\cdot P^{F,s}_{l,t}\cdot S^{F_P,s}_{l,t} + 2\cdot Q^{F,s}_{l,t}\cdot S^{F_Q,s}_{l,t}\right)\cdot\frac{x_l}{V^2_{l\_e,t}},\quad \forall i\in\Omega_N,\forall l\in\Omega_L \qquad (23)$$

where $P^{L,s}_{l,t}$ and $Q^{L,s}_{l,t}$ are the active and reactive power losses of branch l at time t in scenario s. $P^{F,s}_{l,t}$ and $Q^{F,s}_{l,t}$ are the active and reactive power flows through branch l at time t in scenario s. $S^{F_P,s}_{l,t}$ and $S^{F_Q,s}_{l,t}$ are the sensitivity factors of branch flow w.r.t. active power load, and $V_{l\_e,t}$ is the ending bus (downstream) voltage of branch l at time t.

D. Compact Notation

To clearly show the model and facilitate the subsequent expression of the solution methods, a compact notation is applied to elaborate the proposed stochastic bi-level model. The upper level is as follows.

$$min\ 365\cdot\sum_{s\in\Omega_S}\rho_s\cdot g(\boldsymbol{x},s) \qquad (24)$$

$$s.t.\ \boldsymbol{A}\cdot\boldsymbol{x}\le\boldsymbol{b} \qquad (25)$$

$$365\cdot\sum_{s\in\Omega_S}\rho_s\cdot\Pi(\boldsymbol{x},s)\le\boldsymbol{d} \qquad (26)$$

where $\boldsymbol{x}\in\mathbb{Z}^{p_1}_+\times\mathbb{R}^{n_1-p_1}_+$ are the decision variables, including DG units' location and capacity. p_1 and n_1 are the number of candidate buses for installing DG units and the number of total decision variables. $g(\boldsymbol{x},s)$ represents the function of the power loss w.r.t decision variables and scenarios. Equation (25) represents constraints (3) – (5), $\boldsymbol{A}\in\mathbb{R}^{m_1\times n_1}_+$, $\boldsymbol{b}\in\mathbb{R}^{m_1}_+$, and m_1 is the number of constraints in (3) – (5). Equation (26) represents constraint (6), $\boldsymbol{d}\in\mathbb{R}^N_+$, and N is the number of buses in the distribution system. $\Pi(\boldsymbol{x},s)$ represents the function of the energy burden w.r.t decision variables and scenarios.

The lower level is given by:

$$min\ \{\Pi(\boldsymbol{x},s)\} = \min\ h(\boldsymbol{z},\boldsymbol{x},s) \qquad (27)$$

$$s.t.\ \boldsymbol{W}(s)\cdot\boldsymbol{z}\le\boldsymbol{U}(s) - \boldsymbol{Y}(s)\cdot\boldsymbol{x} \qquad (28)$$

where $\boldsymbol{z}$ is the dependent variable affected by $\boldsymbol{x}$, including bus voltage, active power output and reactive power output,$\boldsymbol{z}\in$

$\mathbb{R}_+^{n_3}$, $n_3 = 3 \cdot N - 2$. Equation (28) represents constraints (8)–(15), $\boldsymbol{W} \in \mathbb{R}_+^{m_2 \times n_3}$, $\boldsymbol{U} \in \mathbb{R}_+^{m_2}$, $\boldsymbol{Y} \in \mathbb{R}_+^{m_2 \times n_1}$, and m_2 is the number of constraints in (8)–(15).

III. Scenario Extraction and Variable Nodal Loads

In the stochastic bi-level model, the energy burden constraint is determined by the DLMP. The DLMP is affected by the locational marginal price (LMP) of the wholesale market and nodal loads in the distribution system. However, the LMP and nodal loads vary every hour. If all historical data is considered, the stochastic bi-level model will be difficult or even impossible to solve. Therefore, extracting several scenarios from historical data to present all scenarios is a viable method.

A. Scenario Extraction

Although the wholesale LMP and nodal loads are dynamic, the electricity consumption of households has a certain inertia. Further, the nodal loads are influenced by the climate. Therefore, we may select the average LMP and average nodal loads of each quarter (i.e., season) as the typical scenario of the quarter for this planning problem. That is, four scenarios are extracted, and each scenario consists of LMP data and nodal load data. In terms of the probability of each scenario, it is the ratio of the number of days in the quarter to the total number of days in a year, as shown in (29).

$$\rho_s = \frac{N_s^D}{365}, \forall s \in \Omega_S \tag{29}$$

where N_s^D is the number of days in the quarter s.

B. Variability in Nodal Loads

In the distribution system, it is difficult to forecast the nodal load of each bus [26]. Therefore, it is assumed that there are the same normalized active and reactive load profiles for nodal loads and the whole system load in each scenario [22], [30]. Additionally, to simulate the randomness of the nodal load, a random multiplier is applied to each nodal load.

$$P_{i,t}^{D,s} = \tau_{i,t}^s \cdot M_{i,t}^P \cdot P_t^{D,s}, \forall i \in \Omega_N \tag{30}$$

$$Q_{i,t}^{D,s} = \tau_{i,t}^s \cdot M_{i,t}^Q \cdot Q_t^{D,s}, \forall i \in \Omega_N \tag{31}$$

where $\tau_{i,t}^s$ is the random multiplier of scenario s, which follows a normal distribution, $\tau_{i,t}^s \sim N(1, 0.04^2)$ [30]. $M_{i,t}^P$ and $M_{i,t}^Q$ are normalized active and reactive load profiles, respectively. $P_t^{D,s}$ and $Q_t^{D,s}$ are the active and reactive loads of the whole distribution system in scenario s.

IV. Solution Method

The mathematical solution methods for the proposed stochastic bi-level model include two steps, which are discussed in this section. First, the KKT optimality conditions are applied to convert the stochastic bi-level problem to a single-level problem, i.e., obtaining a stochastic mixed-integer programming (SMIP). The big-M method is used to convert some nonlinear constraints into linear constraints. Then, after performing the time decomposition, the SMIP problem is solved by PHA, which decomposes the original problem into multiple easy-to-solve subproblems, reducing the dimension of the original problems.

A. Solving the Stochastic Bi-Level Problem

The model of the lower level is a convex optimization problem. Therefore, its optimum can be obtained by solving the KKT optimality conditions [31]. Then, the original stochastic bi-level problem can be converted to a single-level problem when the KKT conditions are included as constraints in the upper level. The single-level problem is a SMIP problem, which can be expressed as follows.

$$min\ (2) \tag{32}$$

$$s.t.\ \text{constraints (3)-(6), (8)-(10), (17)-(23), (29)-(31)} \tag{33}$$

$$\sigma_{i,t}^{P,s} - \lambda_t^{P,s} \cdot \left(1 - \frac{\partial P_t^{L,s}}{\partial P_{i,t}^{G,s}}\right) - \sum_{j \in \Omega_N} Z_{j,i}^P \cdot \left(\omega_{j,t}^{v\min,s} - \omega_{j,t}^{v\max,s}\right) + \lambda_t^{Q,s} \cdot \frac{\partial Q_t^{L,s}}{\partial P_{i,t}^{G,s}} - \omega_{i,t}^{P\min,s} + \omega_{i,t}^{P\max,s} = 0, \forall i \in \Omega_G \tag{34}$$

$$\sigma_{i,t}^{Q,s} - \kappa_{i,t}^{-,s} - \kappa_{i,t}^{+,s} = 0, \forall i \in \Omega_G \tag{35}$$

$$-\lambda_t^{Q,s} \cdot \left(1 - \frac{\partial Q_t^{L,s}}{\partial Q_{i,t}^{G,s}}\right) - \sum_{j \in \Omega_N} Z_{j,i}^Q \cdot \left(\omega_{j,t}^{v\min,s} - \omega_{j,t}^{v\max,s}\right) + \lambda_t^{P,s} \cdot \frac{\partial P_t^{L,s}}{\partial Q_{i,t}^{G,s}} - \omega_{i,t}^{Q\min,s} + \omega_{i,t}^{Q\max,s} - \kappa_{i,t}^{-,s} + \kappa_{i,t}^{+,s} = 0, \forall i \in \Omega_G \tag{36}$$

$$0 \le \omega_{i,t}^{v\min,s} \perp \left(V_{i,t}^s - V^{\min}\right) \ge 0, \forall i \in \Omega_N \tag{37}$$

$$0 \le \omega_{i,t}^{v\max,s} \perp \left(V^{\max} - V_{i,t}^s\right) \ge 0, \forall i \in \Omega_N \tag{38}$$

$$0 \le \omega_{i,t}^{P\min,s} \perp \left(P_{i,t}^{G,s} - P_i^{G,\min}\right) \ge 0, \forall i \in \Omega_G \tag{39}$$

$$0 \le \omega_{i,t}^{P\max,s} \perp \left(P_i^R - P_{i,t}^{G,s}\right) \ge 0, \forall i \in \Omega_G \tag{40}$$

$$0 \le \omega_{i,t}^{Q\min,s} \perp \left(Q_{i,t}^{G,s} - Q_i^{G,\min}\right) \ge 0, \forall i \in \{\Omega_G, \Omega_{SC}\} \tag{41}$$

$$0 \le \omega_{i,t}^{Q\max,s} \perp \left(P_{i,t}^{G,s} \cdot \tan(\arccos\alpha_i) - Q_{i,t}^{G,s}\right) \ge 0, \forall i \in \Omega_G \tag{42}$$

$$0 \le \omega_{i,t}^{Q\max,s} \perp \left(Q_i^{G,\max} - Q_{i,t}^{G,s}\right) \ge 0, \forall i \in \Omega_{SC} \tag{43}$$

$$0 \le \kappa_{i,t}^{-,s} \perp \left(\widehat{Q}_{i,t}^{G,s} + Q_{i,t}^{G,s}\right) \ge 0, \forall i \in \Omega_G \tag{44}$$

$$0 \le \kappa_{i,t}^{+,s} \perp \left(\widehat{Q}_{i,t}^{G,s} - Q_{i,t}^{G,s}\right) \ge 0, \forall i \in \Omega_G \tag{45}$$

where (34)–(36) are the stationary conditions. Equations (37)–(45) are the complementary slackness conditions, which are used to deal with the inequality constraints (11)–(15). Here, $0 \le \chi_1 \perp \chi_2 \ge 0$ means that χ_1 and χ_2 satisfy the condition $\chi_1 \ge 0, \chi_2 \ge 0,$ and $\chi_1 \cdot \chi_2 = 0$.

The complementary slackness conditions (37)–(45) are nonlinear, which will make the solution very difficult. To address this challenge, the big-M method is applied. Then, each complementary slackness condition is reformulated as follows.

$$0 \le \chi_1 \le M \cdot \xi, 0 \le \chi_2 \le M \cdot (1 - \xi) \tag{46}$$

where M is a big number, and ξ is a binary variable.

After the substitution, the SMIP model is presented as:

$$min\ (2) \tag{47}$$

$$s.t.\ \text{constraints (33)–(36), (46)} \tag{48}$$

B. Time Decomposition and Progressive Hedging Algorithm

According to the method in Section III, a finite number of scenarios with corresponding probabilities have been obtained. Therefore, the model in (47)–(48) can be regarded as a deterministic mixed-integer nonlinear programming (MINLP). Since there are many scenarios in the deterministic MINLP, it is difficult to solve by using existing off-the-shelf solvers. In literature, the PHA approach has been proposed to solve stochastic mixed-integer problems [32], [33]. Therefore, PHA is used to decompose the model (47)–(48) into scenario-based subproblems and solve them in parallel.

However, the subproblem is also difficult to solve even if it is independent of the scenario. Because there are lots of variables and constraints, including some nonlinear ones, in each subproblem. Thus, based on the Sample Average Approximation method [34], the subproblem-independent scenarios are further decomposed into smaller subproblems that are independent of time. In this paper, Δt is selected as the unit time interval, and the total time interval T is divided into N_T time intervals. Each time interval of one scenario is a smaller subproblem. Considering the quadratic relation between nodal load and objective function as well as energy burden, the probability of each time interval is calculated based on the nodal load, as shown in (49). Then, the probability of each subproblem is the probability of each time interval multiplied by the probability of the corresponding scenario because the time decomposition is performed based on each scenario.

$$\rho_t^s = \frac{\left(\sum_{i\in\Omega_N} P_{i,t}^{D,s}\right)^2}{\sum_{t\in\Omega_T}\left(\sum_{i\in\Omega_N} P_{i,t}^{D,s}\right)^2}, \forall t \in \Omega_T \tag{49}$$

$$\rho'^s_t = \rho_t^s \cdot \rho_s \tag{50}$$

where ρ_t^s is the probability of time t in scenario s, and ρ'^s_t is the probability of the subproblem $t + (s-1)\cdot N_T$.

After the above analysis, the original SMIP problem can be converted to the following problem. Then, we may apply the PHA to solve the model (51)–(53) and solve the obtained subproblems in parallel, which reduces the requirements on computer memory and speeds up the solution.

$$min\ 365\cdot N_T \cdot \sum_{s'\in\Omega_{S'}}\sum_{i\in\Omega_L} \rho'^s_t \cdot P_{i,t}^{L,s} \tag{51}$$

$$s.t.\ 365\cdot N_T \cdot \sum_{s'\in\Omega_{S'}} \rho'^s_t \cdot \frac{\pi_{i,t,s}\cdot P_{i,t}^{D,s}}{I_i} \le e_i^0, \forall i \in \Omega_H \tag{52}$$

$$\text{constraints (3)-(5), (8)-(10), (17)-(23), (29)–(31), (34)–(36), (46)} \tag{53}$$

where $s' = t + (s-1)\cdot N_T$, $\Omega_{S'} = \Omega_S \times \Omega_T$.

The detailed overall solution process is shown in **Algorithm 1**. It should be noted that there are two convergence criteria: (1) each integer variable (i.e., DG location) of all subproblems is identical, and (2) the variation of the continuous variables (i.e., the rated power of installed DG) of all subproblems does not exceed the set threshold.

Algorithm 1 Overall Solution Process

1. Conversion of stochastic bi-level problem: Use KKT condition to convert the stochastic bi-level problem to a single-level problem, i.e., (47) – (48).

2. Decomposition: Perform the time decomposition, the original model can be reformulated as:

$$min\ 365\cdot N_T \cdot \sum_{s'\in\Omega_{S'}} \rho'^s_t \cdot g(\boldsymbol{x}, s')$$

$$s.t.\ 365\cdot N_T \cdot \sum_{s'\in\Omega_{S'}} \rho'^s_t \cdot \Pi(\boldsymbol{x}, s') \le \boldsymbol{d}$$

$$\boldsymbol{A}\cdot\boldsymbol{x} \le \boldsymbol{b}$$

$$\boldsymbol{W}'(s')\cdot\boldsymbol{z}' \le \boldsymbol{U}'(s') - \boldsymbol{Y}'(s')\cdot\boldsymbol{x}$$

$$\boldsymbol{\psi}(s')\cdot\boldsymbol{z}' \le \boldsymbol{\varphi}(s')$$

where $s' = t + (s-1)\cdot N_T$.

3. Initialization: Let $\zeta \leftarrow 0$ and $\boldsymbol{\varpi}_{s'}^{\zeta} \leftarrow 0$, $\forall s' \in \Omega_{S'}$. For each $s' \in \Omega_{S'}$, compute:

$$\boldsymbol{x}_{s'}^{\zeta} \in arg\ min\ g(\boldsymbol{x}, s')$$

$$s.t.\ \Pi(\boldsymbol{x}, s') \le \boldsymbol{d}^{s'}$$

$$\boldsymbol{A}\cdot\boldsymbol{x} \le \boldsymbol{b}$$

$$\boldsymbol{W}'(s')\cdot\boldsymbol{z}' \le \boldsymbol{U}'(s') - \boldsymbol{Y}'(s')\cdot\boldsymbol{x}$$

$$\boldsymbol{\psi}(s')\cdot\boldsymbol{z}' \le \boldsymbol{\varphi}(s')$$

4. Iterative Update: $\zeta \leftarrow \zeta + 1$

5. Aggregation: $\widehat{\boldsymbol{x}}^{\zeta} \leftarrow \sum_{s'\in\Omega_{S'}} \rho'^s_t \cdot \boldsymbol{x}_{s'}^{\zeta-1}$

6. Price Update: $\boldsymbol{\varpi}_{s'}^{\zeta} \leftarrow \boldsymbol{\varpi}_{s'}^{\zeta-1} + \sigma\cdot(\boldsymbol{x}_{s'}^{\zeta-1} - \widehat{\boldsymbol{x}}^{\zeta})$

7. Iteration: For each $s' \in \Omega_{S'}$, compute:

$$\boldsymbol{x}_{s'}^{\zeta} \in arg\ min\left\{g(\boldsymbol{x}, s') + \left(\boldsymbol{\varpi}_{s'}^{\zeta}\right)^T\cdot\boldsymbol{x} + \frac{\sigma}{2}\cdot\left\|\boldsymbol{x} - \widehat{\boldsymbol{x}}^{\zeta}\right\|^2\right\}$$

$$s.t.\ \Pi(\boldsymbol{x}, s') \le \boldsymbol{d}^{s'}$$

$$\boldsymbol{A}\cdot\boldsymbol{x} \le \boldsymbol{b}$$

$$\boldsymbol{W}'(s')\cdot\boldsymbol{z}' \le \boldsymbol{U}'(s') - \boldsymbol{Y}'(s')\cdot\boldsymbol{x}$$

$$\boldsymbol{\psi}(s')\cdot\boldsymbol{z}' \le \boldsymbol{\varphi}(s')$$

If each binary variable of all subproblems is identical, and the variation of the continuous variables of all subproblems meets the criteria, (i.e., less than the set threshold), then the algorithm ends. Otherwise, go back to Step 4.

V. Case Studies

To illustrate the effectiveness of the proposed model, a simple 18-bus feeder and the IEEE 123-bus system were applied as the test systems. Simulation studies were performed on a Server with Intel Core 6248R CPU and 64GB RAM. MATLAB 2022a was the testing environment for the method, and YALMIP and GUROBI 9.5.2 were used as the solving tool.

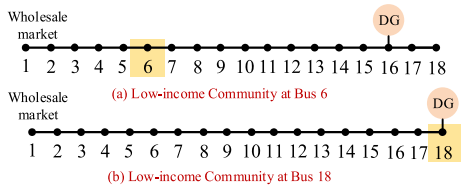

Fig. 2. 18-bus system with a low-income community and a planned DG.

TABLE I
PARAMETERS OF THE 18-BUS SYSTEM

Class	Parameter	Value
System constraints	V^{min}	0.95 p.u.
	V^{max}	1.05 p.u.
	V_{Sub}	1.0 p.u.
	Load in 96 cases (4 scenarios, 24 hours each scenario)	Mean: 2.44 MW + 0.36 MVar Min: 2.07 MW + 0.28 MVar Max: 3.29 MW + 0.52 MVar
Investment constraints	P^{DG}_{max}	3 MW
	N_{DG}	1
	α	\$ 254/kW
	β	\$ 3.18×10^4
	c_{dg}	\$ 1×10^6
	Bidding price	\$ 20/MWh
Shunt capacitor	Location	Bus #13
	Bidding price	\$ 0/ MVarh
	Capacity	0.5 MVar

It should be noted that the DG size does not come at any value; rather, it comes at some discrete value. Here, we have assumed the increment of DG sizes is 100 kW. In the planning model, we have considered their size as a continuous variable but will be rounded to the nearest available size.

A. 18-Bus Feeder System

The topology of the 18-bus distribution feeder, shown in Fig. 2, is employed here for two straightforward case studies to illustrate the fundamental idea and implication of the energy-equity-based DG siting and sizing problem. In this simple feeder, there are 18 load buses and 17 branches. Each bus may correspond to a small community. A shunt capacitor is installed at bus 14, which is used to provide reactive power compensation to regulate bus voltage. The parameters of the 18-bus feeder are listed in TABLE I. The extracted scenarios include LMP patterns and load patterns, shown in Fig. 3.

Two cases with the low-income community at bus 6 and bus 18, respectively, are analyzed and shown in Figs. 2(a) and 2(b). Note, each subfigure also shows the resultant DG location, which is at bus 16 and 18, respectively. More detailed results can be found in the following case study discussions.

1) Low-Income Community at Bus 6:

a) DG siting and sizing results: In this case study, we have assumed that there is a low-income community at bus 6. By solving the model (51) – (53), we can obtain the optimal DG unit siting and sizing results under a specific energy burden constraint. In this case, we first estimate the possible minimum energy burden (MEB) by installing possible DG units. Essentially, the MEB is obtained by solving the following model, i.e., the energy burden of the low-income community is the objective function and other constraints remain.

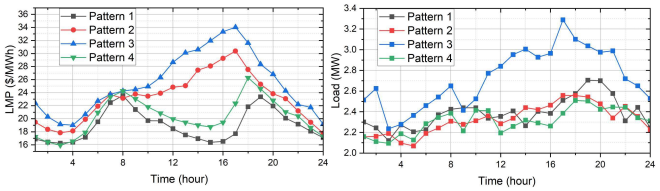

(a) LMP patterns (b) Load patterns

Fig. 3. LMP patterns and load patterns.

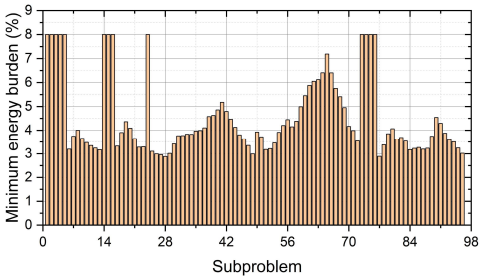

Fig. 4. Minimum energy burden of low-income community at bus 6.

$$\min\ 8760 \cdot \sum_{i\in\Omega_{LH}} \sum_{s'\in\Omega_{S'}} \rho'^{s}_{t} \cdot \frac{\pi_{i,t,s} \cdot P^{D,s}_{i,t}}{I_i} \tag{54}$$

$$s.t.\ \text{constraint (53)} \tag{55}$$

Based on the time decomposition and PHA method, the original SMIP is decomposed into 96 subproblems ($\Delta t = 1,\ T = 24,\ N_T = 24$). Therefore, 96 MEB values are obtained by solving each subproblem of the model (54)–(55) separately, as shown in Fig. 4. The MEB value being 8% means that no optimization is required at this subproblem. Because the DLMP is lower than the bidding price of the DG units. It can be observed that the MEB value varies with the subproblems. The reason is that the load value and DLMP in different subproblems are different.

To make sure the original problem is solvable, the value of 1.01*MEB is selected as the energy burden constraint. The optimal DG unit siting and sizing results are obtained, and one DG unit with rated power of 2.5 MW is installed at bus 16, as shown in Fig. 2(a).

Fig. 5 and Fig. 6 show the branch power losses and bus voltage of two cases without and with DG units, respectively. The power losses of the upstream branch decrease and the power losses of the downstream branch increase, because the installed DG unit at bus 16 changes the power flow. Overall, the accumulated annual power losses of the whole feeder decrease from 1015.63 MWh to 551.03 MWh (i.e., hourly average losses reduce from 115.94 kWh to 62.90 kWh). In addition, it can be observed from Fig. 6 that the voltages of all buses are improved. The reason is that the reduced branch flow and reduced power losses decrease voltage drop. This is a reasonable and expected result.

Since the energy burden is a composite value over the course of a year, the new energy burden of each community (i.e., at each node) is re-optimized after installing the DG unit at bus 16. Fig. 7 shows the percentage reduction in energy burden

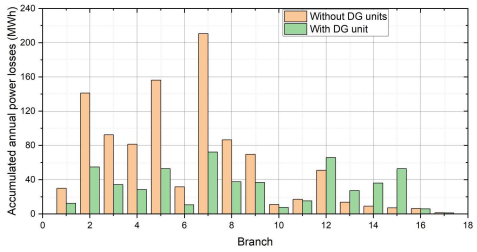

Fig. 5. Branch power losses in one year.

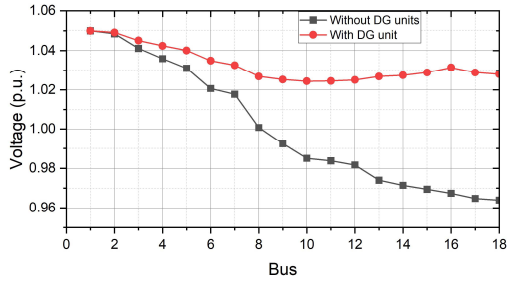

Fig. 6. Average bus voltage in one year.

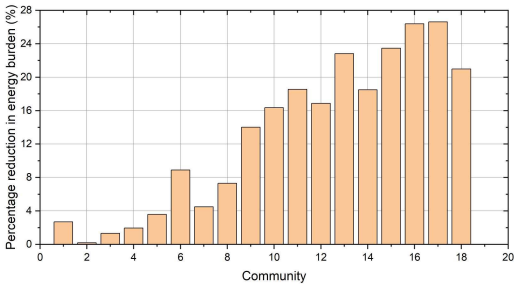

Fig. 7. Percentage reduction in energy burden of each community.

for each community after installing DG units. The energy burden of the low-income community at bus 6 decreased by 8.90% w.r.t. the original average energy burden value. Other communities' energy burden values are also reduced. The reason is that installation of a DG unit changes the power flow, reduces the power losses, and improves the bus voltage. This reduces the DLMP or payment of each community. In addition, the percentage reduction in energy burden for the community at bus 6 located upstream of the distribution feeder is not the largest one. Because installing DG units reduces the DLMP of buses by reducing the marginal power loss price and the marginal voltage support price, and the DLMP of buses located in the downstream of the distribution feeder can be more affected by these two parts than that of buses located in the upstream. Therefore, this free-ride scenario is possible when planners intend to improve energy equity at a specific location to meet the energy burden criterion. This observation is very similar to reliability improvement projects which may give a free-ride to other consumers.

b) Effect of energy equity: Table II shows the results of different cases with different energy burden constraints. Although the DG unit is installed at the same bus in different cases, the rated power of the installed DG units is different. It can be seen from Table II that as the value of the energy

TABLE II
RESULTS OF CASES WITH DIFFERENT ENERGY BURDEN VALUE ON THE 18-BUS SYSTEM WITH LOW-INCOME COMMUNITY AT BUS 6

Different cases	1.01*MEB	1.02*MEB	1.10*MEB	1.50*MEB
DG unit bus (#)	16	16	16	16
Rated power of DG units (MW)	2.5	2.0	1.8	1.8
Power losses (MWh)	551.03	509.66	473.30	473.30
Energy burden of low-income community (%)	3.86	3.89	3.91	3.91
Additional cost ($)	2330.42	1054.40	0	0

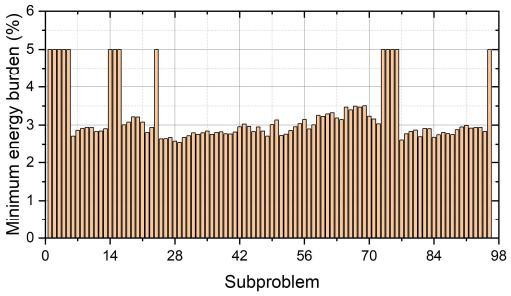

Fig. 8. Minimum energy burden of low-income community at bus 18.

burden constraint increases (i.e., the energy burden constraint not being binding), the power losses of the whole system gradually decrease. It should be noted that the binding energy burden constraint causes smaller feasible regions for the optimization problem, thus we will achieve a worse objective function than the case without energy burden considered.

In addition, the energy burden of the low-income communities will be higher if the energy burden constraint is not binding. The energy burden of low-income communities in the case without any binding energy burden constraint is 3.91%, which is lower than that in the case without DG unit, i.e., 4.09%. This observation shows that installing DG units can reduce the energy burden of communities over a long period of time.

The additional cost is the generation cost from higher power losses, which is based on the power losses in the case with no binding energy burden constraint. Clearly, the case with the smallest value of energy burden constraint has the largest additional cost.

2) Low-Income Community at Bus 18:

a) DG siting and sizing results: In this case study, we have assumed that there is a low-income community at bus 18. Based on the previous case with a low-income community at bus 6, the nodal load at bus 6 and bus 18 is swapped with each other, and all other buses' load remains unchanged. Fig. 8 shows the MEB of this case, which is obtained by solving 96 subproblems of the model (54)–(55). The subproblem with an MEB value of 5% does not have to be solved, because the DLMP is lower than the DG unit's bidding price.

In this case, the model with energy burden constraint being 1.0001*MEB is solved. The optimal DG unit siting and sizing result is installing one DG unit with a rated power of 2.1 MW at bus 18, the same location as the low-income community. This is shown in Fig. 2(b). The branch power losses of cases

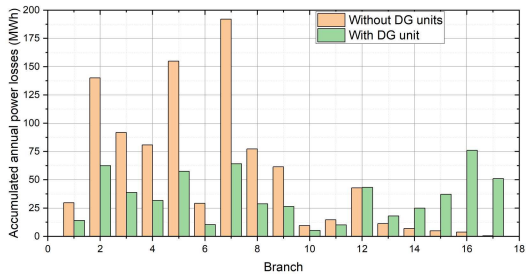

Fig. 9. Branch power loss in one year.

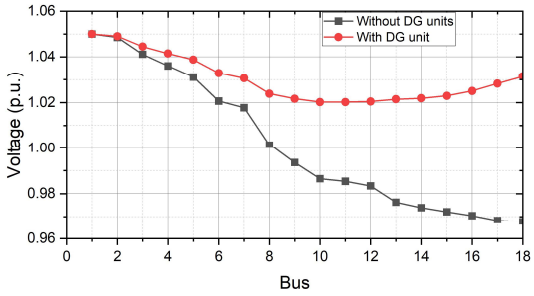

Fig. 10. Average bus voltage in one year.

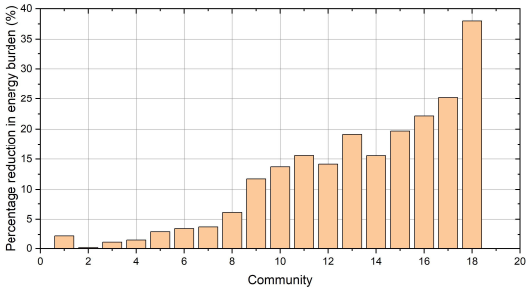

Fig. 11. Percentage reduction in energy burden of each community.

without and with DG units are shown in Fig. 9. Since the power flow is changed by the installed DG units, the power loss of the upstream branches $\Omega_{NB} = \{1, 2, \ldots, 11\}$decreases, while the power loss of the downstream branches $\Omega_{NB} = \{13, 14, \ldots, 17\}$ increases. The accumulated annual power losses of the whole feeder decrease from 952.00 MWh to 599.73 MWh (i.e., hourly average losses reducing from 108.68 kWh to 68.46 kWh). Fig. 10 shows the average bus voltage of two cases, without and with DG units. The voltages of all buses increase because of the reduced power losses. Again, this is reasonable and expected.

The percentage reduction in energy burden of each community after installing DG units is shown in Fig. 11. Evidently, the energy burden of low-income community at bus 18 is greatly reduced and other communities' energy burden also decreases. The reason is that the DLMP of communities decrease with the reduced power losses and bus voltage deviation. Therefore, the electricity bill decreases and the energy burden decreases. The low-income community in this case is at the downstream end of the distribution feeder, i.e., bus 18, and its percentage reduction in energy burden is the largest one.

TABLE III
RESULTS OF CASES WITH DIFFERENT ENERGY BURDEN VALUE ON THE 18-BUS SYSTEM WITH LOW-INCOME COMMUNITY AT BUS 18

Different cases	1.0001*MEB	1.003*MEB	2*MEB	2.5*MEB
DG unit bus (#)	18	17	16	16
Rated power of DG units (MW)	2.1	2.1	2.3	2.3
Power losses (MWh)	599.73	582.88	544.92	544.92
Energy burden of low-income community (%)	2.88	2.89	2.91	2.91
Additional cost ($)	1321.20	936.43	0	0

b) Effect of energy equity: The results of different cases with different energy burden constraints are shown in Table III.

From Table III, there are different DG unit locations and rated power in different cases. The power losses and additional cost decrease if the energy burden value in constraint is relaxed (i.e., being a larger value). But the final energy burden of the low-income community gradually increases, because the binding constraint decreases the feasible region of this optimization model. Similar to the previous case with the low-income community at bus 6, although the energy burden constraint is not binding in the optimization model, the final energy burden of community 18 is still lower than that of the case without installing DG units.

3) Guidelines Obtained From the 18-Bus Feeder System: By a comparison of the two 18-bus system case studies, the following conclusions can be obtained, which can be regarded as general guidelines for DG siting and sizing problems considering energy equity.

- If the low-income community is located in the downstream section of a distribution feeder, DG units tend to be installed near this community because this will significantly reduce the DLMP and thus energy burden, meanwhile improving distribution voltages. In contrast, if the low-income community is not in the downstream of the feeder, DG units may not be installed near the community due to technical constraints like voltage requirement.
- Different energy burden requirements (i.e., energy burden values in optimization constraint) lead to different economic costs, which can be calculated by the model and solution method proposed in this paper.
- Under the same investment conditions, installing DG units reduces the energy burden more significantly for low-income communities located in the downstream of the feeder. Thus, planners may give higher priority to these downstream low-income communities if many similar low-income ones spread out within the same feeder.

B. IEEE 123-Bus System

1) System Description: Fig. 12 shows the topology of the modified IEEE 123-bus system. There are four buses $\Omega_{SC} = \{46, 75, 94, 109\}$ with shunt capacitors to regulate the voltage of this system. Communities at bus $\Omega_{LH} = \{51, 83, 96, 114\}$ are assumed to be low-income. The parameters of this system

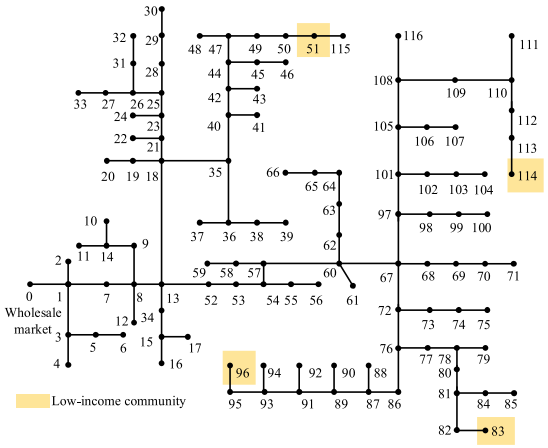

Fig. 12. Modified IEEE 123-bus system.

TABLE IV
PARAMETERS OF THE MODIFIED IEEE 123-BUS SYSTEM

Class	Parameter	Value
System constraints	Low-income community location	Bus # 51, 83, 96,114
	V^{min}	0.95 p.u.
	V^{max}	1.05 p.u.
	V_{Sub}	1.0 p.u.
	Load in 96 cases (4 scenarios, 24 hours each scenario)	Mean: 6.00 MW + 1.45 MVar Min: 5.00 MW + 1.16 MVar Max: 7.69 MW + 2.08 MVar
Investment constraints	P_{max}^{DG}	2 MW
	N_{DG}	5
	α	\$ 254/kW
	β	\$ 3.18×10^4
	c_{dg}	\$ 1×10^7
	Bidding price	\$ 20/MWh
Shunt capacitor	Location	Bus # 46,75,94,109
	Bidding price	\$ 0/ MVarh
	Capacity	0.5 MVar

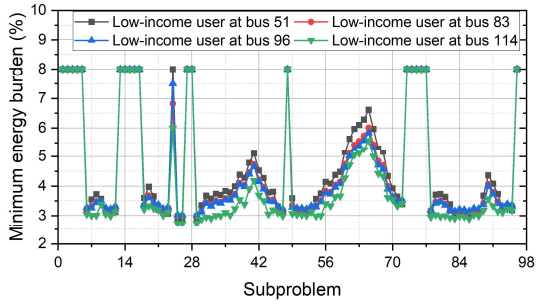

Fig. 13. Minimum energy burden of low-income communities.

are listed in Table IV. Additionally, the LMP patterns of extracted scenarios are the same as that in the 18-bus feeder system, and corresponding load patterns are obtained.

2) DG Siting and Sizing Results: Through solving subproblems of model (54)–(55), the MEB of four low-income communities is obtained, as shown in Fig. 13. The subproblem with an MEB of 8% means that its DLMP is lower than the DG units' bidding price and the energy burden constraint is always satisfied.

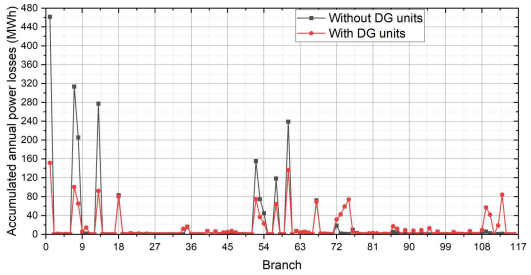

Fig. 14. Branch power loss in one year.

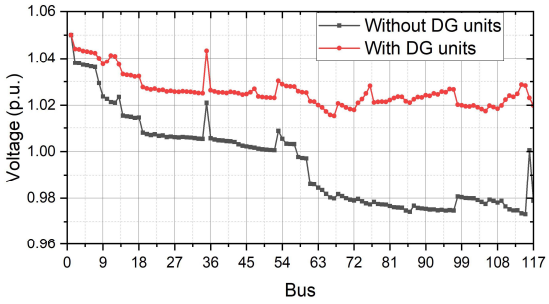

Fig. 15. Average bus voltage in one year.

The 1.05*MEB is selected as the energy burden constraint for ensuring the solvability of the bi-level model. The optimal strategy is to install DG units on bus $\Omega_{dG} = \{35, 76, 83, 96, 114\}$, and with rated power of 0.8 MW, 1.6 MW, 0.7 MW, 1.6 MW, and 1.6 MW, respectively. Fig. 14 shows the branch power losses of two cases without DG units and with DG units. It is evident that the power losses on the branch $\Omega_{NB} = \{1, 8, 9, 13, 18, 52, 53, 54, 57, 60\}$ greatly decrease, the power losses on the branch $\Omega_{NB} = \{72, 86, 87, 89, 96, 108, 109, 110, 112, 113, 114\}$ increase slightly. Overall, the accumulated annual power losses of the whole system decrease from 2201.20 MWh to 1532.47 MWh (i.e., hourly average losses reduce from 251.28 kWh to 174.94 kWh). This is because installation of DGs reduces the branch flows in general.

The average bus voltages of two cases without DG units and with DG units are shown in Fig. 15. It can be seen that the voltage of each bus is greatly improved. The reason is that the voltage drop on branches decreases as the power through the branch decreases and the power losses reduce as well.

Fig. 16 shows the percentage reduction in energy burden of each community after installing DG units. Evidently, the energy burden of low-income communities is reduced by {4.20%, 14.18%, 14.98%, 17.05%}, and other communities' energy burden is also reduced. Because installed DG units decrease the DLMP by reducing power losses and improving bus voltages, which reduces communities' electricity bills. Additionally, the energy burden of low-income communities at buses 83, 96, 114 decreased significantly, but the energy burden of community at bus 51 decreased slightly. The reason is that bus 51 is relatively located upstream of the system and the decrease of its DLMP is smaller. This is consistent with the observation from the studies of the 18-bus feeder.

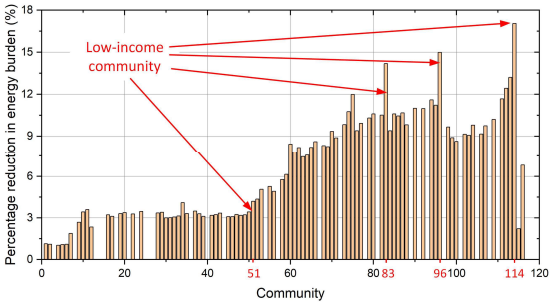

Fig. 16. Percentage reduction in energy burden of each community.

TABLE V
RESULTS OF CASES WITH DIFFERENT ENERGY BURDEN VALUE ON THE MODIFIED IEEE 123-BUS SYSTEM

Different cases	1.05*MEB	1.08*MEB	1.3*MEB	1.7*MEB
DG unit bus (#)	35, 76, 83, 96, 114	35, 65, 76, 96, 114	35, 65, 76, 90, 114	35, 65, 76, 90, 114
Rated power of DG units (MW)	0.8, 1.6, 0.7, 1.6, 1.6	1.5, 0.5, 1.6, 1.0, 1.6	1.6, 1.6, 1.6, 0.5, 0.9	1.6, 1.6, 1.6, 0.5, 0.9
Power losses (MWh)	1532.47	1432.50	1100.20	1100.20
Energy burden of low-income communities (%)	3.66, 3.65, 3.47, 3.11	3.67, 3.73, 3.54, 3.14	3.64, 3.73, 3.56, 3.20	3.64, 3.73, 3.56, 3.20
Additional cost ($)	10784	8207.9	0	0

3) Effect of Energy Equity: When the value of the energy burden constraint changes, different results are obtained, as shown in Table V. It can be seen from Table V that smaller energy burden constraint causes lower power losses, a larger final energy burden, and less additional cost. Also, the low-income community's final energy burden value {3.64%, 3.73%, 3.56%, 3.20%} in the case with 1.7*MEB constraint is lower than that of the case without DG units, i.e., {3.79%, 4.07%, 3.91%, 3.61%}. This is because DG unit installation reduces electricity bills for a period of time. Additionally, if comparing the DG units' buses in two cases of 1.05*MEB and 1.08*MEB, we can also obtain the following: for low-income communities at the downstream of a distribution system, DG units will be installed near the community when the energy burden constraint is binding. However, for low-income communities which are not on the downstream of the system, there is no pressing need to install DG units near the low-income community. This is consistent with the observations from the studies of the 18-bus feeder.

C. Performance Analysis of Solution Method

1) Computation Time: Table VI shows the computation time of different cases. The computation time used by Cplex or Gurobi to directly solve the coupling problem is NA (out-of-memory error), which means the result cannot be obtained if these two solvers are directly employed to solve the original coupling problem. However, the result can be obtained by the proposed solution method. Although the solution time for the 123-bus system is somewhat long, it remains acceptable given the offline nature of this planning problem.

TABLE VI
COMPUTATION TIME OF DIFFERENT CASES

Different cases	Low-income community at bus 6	Low-income community at bus 18	123-bus system
Computation time used by Cplex or Gurobi to directly solve the coupling problem	NA (Out-of-memory error)	NA (Out-of-memory error)	NA (Out-of-memory error)
Computation time used by the proposed solution method (min)	2.93	2.75	115.53

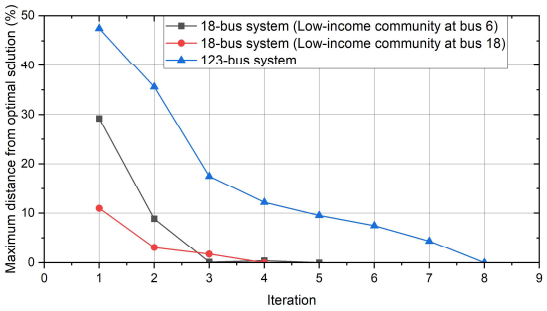

Fig. 17. Convergence curve of different feeder cases.

TABLE VII
ERROR OF DIFFERENT CASES

Different cases	18-bus (Low-income community at bus 6)	18-bus (Low-income community at bus 18)
Optimal strategy obtained by enumeration method	DG unit bus is #16 Rated power is 2.5 MW	DG unit bus is #18 Rated power is 2.1 MW
Optimal strategy obtained by the proposed solution method	DG unit bus is #16 Rated power is 2.5 MW	DG unit bus is #18 Rated power is 2.1 MW
Error	0	0

2) Convergence Performance: The maximum distance between solutions in iterations and the optimal solution of different cases is shown in Fig. 17. Evidently, the distance forms a decreasing sequence, which is consistent with the convergence theorem in [33]. Additionally, the solving of the 18-bus feeder system converges at the 5th and 4th iteration, and the solving of the 123-bus system converges at the 8th iteration.

3) Calculation Error: For analyzing the errors of solution method, the enumeration method is used to obtain solutions for the 18-bus feeder system, then compare results obtained by the enumeration method and proposed solution method. Table VII shows the errors of different cases. Evidently, the calculation error is 0, indicating the optimality of the obtained solutions.

VI. CONCLUSION

In this paper, a stochastic bi-level model is proposed to formulate the DG siting and sizing problem with energy equity constraint modeled by energy burden. Then, the stochastic bi-level model is converted to a single-level model by KKT optimality conditions, and the single-level model is solved by the proposed time decomposition method and PHA. Numerical

studies are performed on an 18-bus distribution feeder and the IEEE 123-bus system, which verifies that installation of DG units is an effective approach to implement energy equity. Further, general guidelines for DG units' siting and sizing problem with energy equity constraint are obtained as follows. Notably, these guidelines hold substantial significance in real-world practice in addressing the DG planning problem, particularly when faced with challenges such as missing measurements, incomplete data, or a lack of analytical resources. Therefore, if a system planner is unable to perform a comprehensive analytical or optimization study, the guidelines outlined below, especially the first and second bullets, can serve as valuable planning references without the need of detailed analysis.

- DG units are not always installed near low-income communities, even considering the energy equity constraint. The decision of whether DG units are installed near low-income communities depends on the communities' location in the system as well as technical constraints.
- When multiple low-income communities are spread throughout a system, it is generally more effective to install DGs near the low-income communities in the downstream of feeders.
- To achieve a lower level of energy burden for low-income communities, a quantitative economic evaluation is needed for accurate siting and sizing such as the proposed method, which is related to the system topology and the location of low-income communities, as well as the technical and energy burden constraints.

In the future, models with different types of DG units, like solar photovoltaics, wind turbines, and battery storages, will be further studied. Also, time-coupling features of devices like battery storages can be studied via decomposition by the Bellman Equation in Markov process approaches or solved by deep learning. Other than DG installation, improvement on distribution system assets like upgrading distribution cables/transformers and installing reactive power compensation facilities may have considerable impacts on energy equity, not only economically but also in the sense of energy service reliability and quality. These can be possible future topics.

REFERENCES

[1] L. V. White and N. D Sintov, "Health and financial impacts of demand-side response measures differ across sociodemographic groups," *Nat. Energy*, vol. 5, pp. 50–60, Jan. 2020.

[2] R. Bryce. "The high cost of California electricity is increasing poverty." 2020. [Online]. Available: https://freopp.org/the-high-cost-of-californiaelectricity-is-increasing-poverty-d7bc4021b705

[3] (U.S. Department of Energy, Washington, DC, USA). *Equity Action Plan Summary: U.S. Department of Energy*. (2021). [Online]. Available: https://www.whitehouse.gov/wp-content/uploads/2022/04/DOE-EO13985-equity-summary.pdf

[4] E. Scheier and N. Kittner, "A measurement strategy to address disparities across household energy burdens," *Nat. Commun.*, vol. 13, p. 288, Jan. 2022.

[5] S. Cong, D. Nock, Y. L. Qiu, and B. Xing, "Unveiling hidden energy poverty using the energy equity gap," *Nat. Commun*, vol. 13, p. 2456, May 2022.

[6] E. D. Fechter-Leggett, A. Vaidyanathan, and E. Choudhary, "Heat stress illness emergency department visits in national environmental public health tracking states, 2005–2010," *J. Community Health*, vol. 41, pp. 57–69, Feb. 2016.

[7] N. Fefferman, C. F. Chen, G. Bonilla, H. Nelson, and C. P. Kuo, "How limitations in energy access, poverty, and socioeconomic disparities compromise health interventions for outbreaks in urban settings," *iScience*, vol. 24, no. 12, Dec. 2021, Art. no. 103389.

[8] C. F. Chen, J. Feng, N. Luke, C.P. Kuo, and J. S. Fu, "Localized energy burden, concentrated disadvantage, and the feminization of energy poverty," *iScience*, vol. 25, no. 4, Mar. 2022, Art. no. 104139.

[9] R. S. Li'evanos, "Racialized structural vulnerability: Neighborhood racial composition, concentrated disadvantage, and fine particulate matter in California," *Int. J. Environ. Res. Public Health*, vol.16, no. 17, p. 3196, Sep. 2019.

[10] D. J. Bednar and T. G. Reames, "Recognition of and response to energy poverty in the United States," *Nat. Energy*, vol. 5, pp. 432–439, Jun. 2020.

[11] (U.S. Dept. Health & Human Services, Washington, DC, USA). *Low Income Home Energy Assistance Program (LIHEAP)*. 2023. [Online]. Available: https://www.acf.hhs.gov/ocs/programs/liheap

[12] E. M. Rose, and B. A. Hawkins, "Background data and statistics on low-income energy use and burden for the weatherization assistance program: Update for fiscal year 2020," Oak Ridge Nat. Lab., Oak Ridge, TN, USA, Rep. ORNL/TM-2020/1566, 2020. [Online]. Available: https://weatherization.ornl.gov/wp-content/uploads/2021/01/ORNL_TM-2020_1566.pdf

[13] "Clean energy targets," Oregon House Bill, 2021. [Online]. Available: https://olis.oregonlegislature.gov/liz/2021R1/Downloads/MeasureDocument/HB2021/Enrolled

[14] "Amendment to senate bill 2408," Illinois, Sep. 2021. [Online]. Available: https://ilga.gov/legislation/102/SB/PDF/10200SB2408ham002.pdf

[15] Y. Chen, M. Tanaka, and R. Takashima, "Energy expenditure incidence in the presence of prosumers: Can a fixed charge lead us to the promised land?" *IEEE Trans. Power Syst.*, vol. 37, no. 2, pp. 1591–1600, Mar. 2022.

[16] Y. Chen, A. L. Liu, M. Tanaka, and R. Takashima, "Optimal retail tariff design with prosumers: Pursuing equity at the expenses of economic efficiencies?" *IEEE Trans. Energy Markets, Policy Reg.*, vol. 1, no. 3, pp. 198–210, Sep. 2023, doi: 10.1109/TEMPR.2023.3293711.

[17] N. Nandasiri and V. Aravinthan, "Equity-based fair market algorithm to effectively integrate DER in retail market pricing," in *Proc. North Amer. Power Symp. (NAPS)*, College Station, TX, USA, 2021, pp. 1–6.

[18] J. Lei et al., "A shareholding-based resource sharing mechanism for promoting energy equity in peer-to-peer energy trading," *IEEE Trans. Power Syst.*, vol. 38, no. 6, pp. 5113–5127, Nov. 2023, doi: 10.1109/TPWRS.2022.3225656.

[19] M. Heleno et al., "Optimizing equity in energy policy interventions: A quantitative decision-support framework for energy justice," *Appl. Energy*, vol. 325, Nov. 2022, Art. no. 119771.

[20] S. H. Lee and J.-W. Park, "Selection of optimal location and size of multiple distributed generations by using Kalman filter algorithm," *IEEE Trans. Power Syst.*, vol. 24, no. 3, pp. 1393–1400, Aug. 2009.

[21] H. Xing, H. Fan, X. Sun, S. Hong, and H. Cheng, "Optimal siting and sizing of distributed renewable energy in an active distribution network," *CSEE J. Power Energy Syst.*, vol. 4, no. 3, pp. 380–387, Sep. 2018.

[22] Q. Shi et al., "Resilience-oriented DG siting and sizing considering stochastic scenario reduction," *IEEE Trans. Power Syst.*, vol. 36, no. 4, pp. 3715–3727, Jul. 2021.

[23] B. Zeng, J. Zhang, X. Yang, J. Wang, J. Dong, and Y. Zhang, "Integrated planning for transition to low-carbon distribution system with renewable energy generation and demand response," *IEEE Trans. Power Syst.*, vol. 29, no. 3, pp. 1153–1165, May 2014.

[24] (U.S. Dept. Energy, Washington, DC, USA). *Low-Income Community Energy Solutions*. [Online]. Available: https://www.energy.gov/scep/slsc/low-income-community-energy-solutions

[25] C. Marnay et al., "Modeling of customer adoption of distributed energy resources," Dept. CERTS Distrib.z Gener. Test Bed Team, Ernest Orlando Lawrence Berkeley Nat. Lab., Berkeley, CA, USA, Rep. LBNL-49582, Aug. 2011. [Online]. Available: https://escholarship.org/uc/item/6ts3c2pd

[26] X. Wang, F. Li, Q. Zhang, Q. Shi, and J. Wang, "Profit-oriented BESS siting and sizing in deregulated distribution systems," *IEEE Trans. Smart Grid*, vol. 14, no. 2, pp. 1528–1540, Mar. 2023.

[27] L. Bai, J. Wang, C. Wang, C. Chen, and F. Li, "Distribution locational marginal pricing (DLMP) for congestion management and voltage support," *IEEE Trans. Power Syst.*, vol. 33, no. 4, pp. 4061–4073, Jul. 2018.

[28] X. Wang, F. Li, L. Bai, and X. Fang, "DLMP of competitive markets in active distribution networks: Models, solutions, applications, and visions," *Proc. IEEE*, vol. 111, no. 7, pp. 725–743, Jul. 2023.
[29] P. Kundur, *Power System Stability and Control*. New York, NY, USA: McGraw-Hill, 1994.
[30] S. Ma, L. Su, Z. Wang, F. Qiu, and G. Guo, "Resilience enhancement of distribution grids against extreme weather events," *IEEE Trans. Power Syst.*, vol. 33, no. 5, pp. 4842–4853, Sep. 2018.
[31] A. J. Conejo and C. Ruiz, "Complementarity, not optimization, is the language of markets," *IEEE Open Access J. Power Energy*, vol. 7, pp. 344–353, 2020.
[32] R. T. Rockafellar and R. J.-B. Wets, "Scenarios and policy aggregation in optimization under uncertainty," *Math. Oper. Res.*, vol. 16, no. 1, pp. 119–147, Feb. 1991.
[33] R. T. Rockafellar, "Solving stochastic programming problems with risk measures by progressive hedging," *Set Valued Var. Anal*, vol. 26, pp. 759–768, Dec. 2018.
[34] B. Verweij, S. Ahmed, A. J. Kleywegt, G. Nemhauser, and A. Shapiro, "The sample average approximation method applied to stochastic routing problems: A computational study," *Comput. Optim. Appl.*, vol. 24, pp. 289–333, Feb. 2003.

Chenchen Li (Graduate Student Member, IEEE) received the B.S.E.E. and M.S.E.E. degrees from North China Electric Power University, Beijing, China, in 2019 and 2022, respectively. She is currently pursuing the Ph.D. degree in electrical engineering with The University of Tennessee, Knoxville, TN, USA. Her research interests include distribution system optimization, distribution system planning, and energy equity in the power system.

Fangxing Li (Fellow, IEEE) is also known as Fran Li. He received the B.S.E.E. and M.S.E.E. degrees from Southeast University, Nanjing, China, in 1994 and 1997, respectively, and the Ph.D. degree from Virginia Tech, Blacksburg, VA, USA, in 2001.

He is currently the John W. Fisher Professor of Electrical Engineering and the Campus Director of the CURENT, The University of Tennessee, Knoxville, TN, USA. His current research interests include renewable energy integration, demand response, distributed generation and microgrid, electricity markets, and power system computing. He has received a number of awards and honors, including IEEE Fellow (Class of 2017), the R&D 100 Award in 2020, the IEEE PES Technical Committee Prize Paper Award in 2019, five best paper awards at international journals, and seven best papers/posters at international conferences. He served as the Chair of IEEE PES Power System Operation, Planning and Economics Committee from 2020 to 2021. He has been serving as the Editor-in-Chief of IEEE OPEN ACCESS JOURNAL OF POWER AND ENERGY since 2020.

Sufan Jiang (Member, IEEE) received the B.S.E.E., M.S.E.E., and Ph.D. degrees from Southeast University, Nanjing, China, in 2014, 2017, and 2022, respectively. He is currently a Research Scientist with The University of Tennessee, Knoxville, TN, USA. His research interests include resilience, flexibility, and energy justice of power systems.

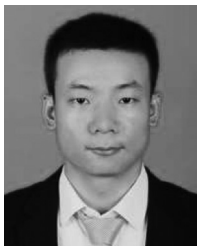

Xiaofei Wang (Member, IEEE) received the B.S.E.E. degree from North China Electric Power University in 2014, China, the M.S.E.E. degree from Wuhan University, China, in 2017, and the Ph.D. degree from The University of Tennessee, Knoxville, TN, USA, in 2023. He is currently a Postdoctoral Researcher with National Renewable Energy Laboratory. His research interests include the electricity market operation, power system resilience, and distributed energy resource integration.

Jinning Wang (Graduate Student Member, IEEE) received the B.S. and M.S. degrees in electrical engineering from the Taiyuan University of Technology, Taiyuan, China, in 2017 and 2020, respectively. He is currently pursuing the Ph.D. degree in electrical engineering with The University of Tennessee, Knoxville, TN, USA. His research interests include data mining, power system modeling, and renewable integration.